Isoscalar giant monopole resonance within the Bohr-Mottelson model

Jun Su,* Long Zhu, and Chenchen Guo
Sino-French Institute of Nuclear Engineering and Technology, Sun Yat-sen University, Zhuhai 519082, China

(Received 17 May 2018; published 21 August 2018)

Background: With the possibility to measure the isoscalar giant monopole resonance (ISGMR) in the short-lived nuclei, the compressibility of the open-shell and exotic nuclei has attracted much attention.
Purpose: The present work is an attempt to develop a semiclassical model to describe the ISGMR and the compressibility of the finite nuclei.
Method: The fluid dynamical reduction of the Boltzmann-Langevin equation was carried out to describe the collective motion of the nucleus [Z. Phys. A 337, 413 (1990); Z. Phys. A **349**, 119 (1994)]. In this work, by including the Skyrme energy density functional, we develop the model and apply it to the ISGMR. Both the self-consistent and linearized methods are used to solve the corresponding Langevin equation.
Results: It is shown that the calculations of the ISGMR energies in this work agree with those by the relativistic mean-field theory and the random phase approximation, and reproduce the general trend of the data. The model only includes the two-body dissipation, and underestimates the width of the ISGMR. Twelve sets of the Skyrme interactions are applied to perform the calculations and study the incompressibility parameters in the leptodermous expansion. The calculated surface parameter K_S within the model is smaller than the extracted value, and decreases linearly over mass number of the nucleus. The calculated values of the symmetry parameter K_τ and the Coulomb parameter K_C agree with the extracted values by fitting the available data for the nuclei from ^{12}C to ^{238}U.
Conclusions: The Bohr-Mottelson model provides a reasonable method to understand the ISGMR in a macroscopic approach.

DOI: 10.1103/PhysRevC.98.024315

I. INTRODUCTION

The giant resonances, which are collective excitations of nucleons, have been objects of theoretical and experimental research of modern nuclear physics over recent decades since it plays a very crucial role in the understanding of the nonequilibrium properties of nuclei and the nuclear force [1,2]. Particularly, the isoscalar giant monopole resonance (ISGMR) has been extensively investigated in a wide range of nuclei, as a valuable tool to study the nuclear incompressibility at the normal density [3–8]. The consensus on the value of the nuclear incompressibility at 230 ± 40 MeV was reached about a decade ago by the investigation of the doubly magic nuclei such as ^{208}Pb [9,10]. Now, the attention has been directed to the novel effects on the ISGMR in open-shell and light nuclei [11].

One of these novel effects consists in the overestimation of the peak energies for the Sn [12] and Cd [13] isotopes by the models, which can reproduce those for ^{90}Zr, ^{144}Sm, and ^{208}Pb [14]. Many attempts were made to calculate the ISGMR in Sn and Cd isotopes. It was found that increasing the value of the symmetry energy at saturation density can decrease the calculated peak energies while keeping the incompressibility constant [15]. The role of pairing in the description of the ISGMR in Sn and Cd isotopes was also pointed out [16]. However, the results were insufficient to explain the experimental data up to now. Other novel effects were found in light nuclei. Microscopic calculations showed that the ISGMR strength distribution exhibits a two-peak structure due to the deformation of the light-mass nuclei [17,18]. Another structure effect was speculated by recent results on the Ca, Zr, and Mo isotopes. Contrary to the general trend going roughly as $A^{-1/3}$, a decreasing energy with increasing mass number was observed when comparing the energies of the ISGMR in ^{90}Zr to those in ^{92}Mo and ^{92}Zr, as well as ^{40}Ca to ^{48}Ca [19]. It was proposed that the calculations with a common effective interaction would not reproduce the mass dependence of the ISGMR energies in Ca isotopes without the addition of nuclear structure effects. Recently, with the possibility to measure the ISGMR in the short-lived nuclei [20], the compressibility of the exotic and neutron-rich nuclei has become an important topic in nuclear structure [21,22].

Microscopic models, such as the random phase approximation (RPA) [23,24] and the relativistic RPA [25,26], have been developed to describe the ISGMR. In principle, the RPA is the small-amplitude limit of a more general time-dependent Hartree-Fock theory. There are already several extended versions, such as the quasiparticle RPA [27] and second RPA [28], which are developed by including the open-shell effect and particle-vibration coupling respectively. The semiclassical treatments of the ISGMR have also been reported, including the isospin-dependent quantum molecular dynamics (IQMD) [29] and the Boltzmann-Uehling-Uhlenbeck (BUU) transport approach [30].

The present work is an attempt to describe the centroid energies of the ISGMR in finite nuclei by a macroscopic model based on the fluid dynamical reduction of the

*sujun3@mail.sysu.edu.cn

Boltzmann-Langevin equation. The paper is organized as follows. In Sec. II, we describe the method. In Sec. III, we present both the results and discussions. Finally, the summaries are given in Sec. IV.

II. THEORETICAL FRAMEWORK

The fluid dynamical reduction of the Boltzmann-Langevin equation was carried out for a situation where the velocity field can be described by a set of N collective variables [31,32]. A set of N coupled Langevin equations is obtained for the collective variables, which constitute a generalization of the Bohr-Mottelson model for the hot nuclei. The degree of freedom of the ISGMR is a collective variable X, and the velocity field reads,

$$\mathbf{u} = \dot{X}\nabla\frac{r^2}{2}. \tag{1}$$

In the case of spherical symmetry, it gives a scaling condition between the density ρ and the collective variable X,

$$\frac{\partial\rho}{\partial X} = -r\frac{\partial\rho}{\partial r} - 3\rho. \tag{2}$$

The Langevin equation for the collective variable X reads,

$$\begin{aligned} M\ddot{X} + \frac{1}{2}\frac{\partial M}{\partial X}\dot{X}^2 + \frac{\partial V}{\partial X} \\ = C(t) - \int_{-\infty}^{t} dt'\gamma(t-t')\dot{X}(t') + \delta F(t), \end{aligned} \tag{3}$$

where M is the inertia parameter,

$$M = m\int d^3\mathbf{r}r^2\rho, \tag{4}$$

and V is the potential energy, which is the sum of the Coulomb and nuclear Skyrme energies. The Coulomb energy is a combination of the direct and exchange terms,

$$\begin{aligned} V_c = \int d^3\mathbf{r}\frac{e^2}{2}\rho_p(\mathbf{r})\int d^3\mathbf{r}'\frac{\rho_p(\mathbf{r}')}{|\mathbf{r}-\mathbf{r}'|}, \\ -\int d^3\mathbf{r}\frac{3e^2}{4}\left(\frac{3}{\pi}\right)^{1/3}[\rho_p(\mathbf{r})]^{4/3}. \end{aligned} \tag{5}$$

The nuclear Skyrme energy can be written as a sum of two-body term V_0, three-body term V_3, effective mass term V_{eff}, finite-range term V_{fin}, spin-orbit term V_{so}, and tensor coupling term V_{sg} [33,34]:

$$\begin{aligned} V &= V_0 + V_3 + V_{\text{eff}} + V_{\text{fin}} + V_{\text{so}} + V_{\text{sg}} \\ &= \int d^3\mathbf{r}(\varepsilon_0 + \varepsilon_3 + \varepsilon_{\text{eff}} + \varepsilon_{\text{fin}} + \varepsilon_{\text{so}} + \varepsilon_{\text{sg}}), \\ \varepsilon_0 &= \frac{t_0}{2}\left(1+\frac{x_0}{2}\right)\rho^2 - \frac{t_0}{2}\left(x_0+\frac{1}{2}\right)\left(\rho_n^2+\rho_p^2\right), \\ \varepsilon_3 &= \frac{t_3}{12}\left(1+\frac{x_3}{2}\right)\rho^{\sigma+2} - \frac{t_3}{12}\left(x_3+\frac{1}{2}\right)\rho^{\sigma}\left(\rho_n^2+\rho_p^2\right), \\ \varepsilon_{\text{eff}} &= \frac{1}{4}\left[t_1\left(1+\frac{x_1}{2}\right) + t_2\left(1+\frac{x_2}{2}\right)\right]\rho(\tau_n+\tau_p) \\ &\quad + \frac{1}{4}\left[t_2\left(x_2+\frac{1}{2}\right) - t_1\left(x_1+\frac{1}{2}\right)\right](\rho_n\tau_n+\rho_p\tau_p), \\ \varepsilon_{\text{fin}} &= \frac{1}{16}\left[3t_1\left(1+\frac{x_1}{2}\right) - t_2\left(1+\frac{x_2}{2}\right)\right](\nabla\rho)^2 \\ &\quad - \frac{1}{16}\left[3t_1\left(x_1+\frac{1}{2}\right) + t_2\left(x_2+\frac{1}{2}\right)\right] \\ &\quad \times [(\nabla\rho_n)^2 + (\nabla\rho_p)^2], \\ \varepsilon_{\text{so}} &= \frac{1}{2}W_0[\mathbf{J}\cdot\nabla\rho + \mathbf{J}_n\cdot\nabla\rho_n + \mathbf{J}_p\cdot\nabla\rho_p], \\ \varepsilon_{\text{sg}} &= -\frac{1}{16}(t_1x_1+t_2x_2)J^2 + \frac{1}{16}(t_1-t_2)\left(J_n^2+J_p^2\right), \end{aligned} \tag{6}$$

where ρ, τ, and J are, respectively, the local nucleon density, kinetic energy density, and spin density. The subscripts n and p correspond to the proton and neutron densities, respectively.

The terms on the right-hand side of Eq. (3) are the dynamical forces. The first term comes from the incompressibility. The second term is the friction force, due to the coherent coupling between the single-particle and collective motion. The last term is the random force due to the interaction of the collective variable with the heat bath.

$$\begin{aligned} C(t) &= 2E_k = 2\int d^3\mathbf{r}\left[\frac{\hbar^2}{2m}(\tau_n+\tau_p)\right], \\ \gamma(t-t') &= \frac{4}{5}AE_F\exp\left[-\frac{(t-t')\pi^2}{32\sigma v_f\rho E_F}\right], \\ \overline{\delta F(t)\delta F(t')} &= \frac{2}{\pi}\sqrt{E_FE^*}\gamma(t-t'), \end{aligned} \tag{7}$$

where A is the mass number, σ is the cross section of nucleon-nucleon scattering, V_f is the Fermi velocity, E_F is the Fermi energy, and E^* is the excitation energy, i.e., the ISGMR energy.

It was shown by the extended Thomas-Fermi model that the kinetic densities and the spin current vector densities can be expressed as the functions of the local density and its gradient [35]. Using the scaling condition [Eq. (2)], one obtains the inertia parameter, the potential energy, and the dynamical force as functions of the collective variable X,

$$\begin{aligned} M &= M^{(0)}e^{2X}, \\ \frac{\partial M}{\partial X} &= 2M^{(0)}e^{2X}, \\ \frac{\partial V}{\partial X} &= -V_c^{(0)}e^{-X} - 3V_0^{(0)}e^{-3X} \\ &\quad - (3+3\sigma)V_3^{(0)}e^{-(3+3\sigma)X} - 5V_{\text{eff}}^{(0)}e^{-5X} \\ &\quad - 5V_{\text{fin}}^{(0)}e^{-5X} - 5V_{\text{so}}^{(0)}e^{-5X} - 5V_{\text{sg}}^{(0)}e^{-5X}, \\ C(t) &= 2E_k^{(0)}e^{-2X}, \\ E_F &= \frac{5}{3A}E_k^{(0)}e^{-2X}. \end{aligned} \tag{8}$$

Here, the superscript "(0)" means the values in the initial equilibrium state. Those values are provided by the Skyrme Hartree-Fock-Bogolyubov (SHFB) model, the code of which is available [36].

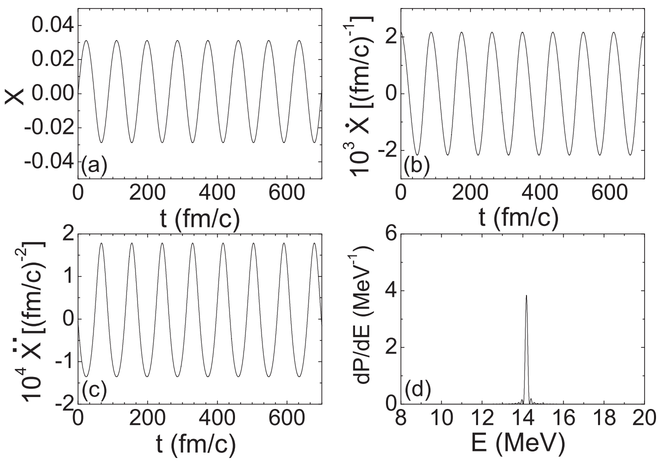

FIG. 1. (a) Time evolution of the collective variable X for ^{208}Pb, (b) the same for velocity $\dot{X}$. (c) the same for acceleration $\ddot{X}$. (d) Frequency spectrum extracted from the acceleration $\ddot{X}$. In the calculation, the friction and random forces are not considered.

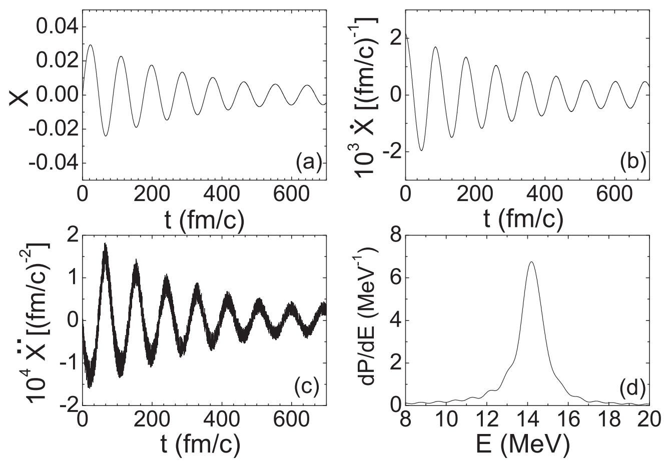

FIG. 2. Same as Fig. 1, but considering the friction and random forces.

III. RESULTS AND DISCUSSIONS

A. Self-consistent solution

The Langevin equation Eq. (3) can be solved self-consistently. The initial value X_0 of the collective variable is the calculated from the equilibrium condition,

$$\frac{\partial V}{\partial X}(X_0) = C(X_0). \tag{9}$$

While, the initial velocity $\dot{X}_0$ depends on the ISGMR energy E^*,

$$\dot{X}_0 = \sqrt{\frac{2E^*}{M^{(0)}}}. \tag{10}$$

Equation (3) without the friction and random forces is solved numerically with the initial conditions. The solution, shown as Figs. 1(a)–1(c), exhibits a good oscillation structure. One sees that the value X_0 in the equilibrium state is 0. The values of the velocity $\dot{X}$ have an order of 10^{-3}, while those of the acceleration $\ddot{X}$ have an order of 10^{-4}. It means that the term related to $\dot{X}^2$ can be ignored.

With the Fourier transform of $\ddot{X}(t)$,

$$\ddot{X}(\omega) = \frac{1}{t_{\max}}\int_0^{t_{\max}} \ddot{X}(t)\exp(-i\omega t)dt, \tag{11}$$

one obtains the frequency spectrum $P(\omega) \propto |\ddot{X}(\omega)|^2$, as shown in Fig. 1(d). Since the damping is not considered, the frequency spectrum shows a narrow peak. The output ISGMR energy $E^*_{\rm out} = \hbar\omega_0$ is calculated by the peak position ω_0 of the frequency spectrum. The output ISGMR energy will be used to calculate the initial velocity $\dot{X}$, and solve the equation again, unless the discrepancy between the input and output ISGMR energy is less than 0.001 MeV.

When the friction and random forces are considered, the time evolution of the collective variable X, its velocity $\dot{X}$, and acceleration $\ddot{X}$ are shown in Figs. 2(a)–2(c). The random force results in the fluctuation of the acceleration $\ddot{X}$. However, its influence on the collective variable X and velocity $\dot{X}$ is weak. Due to the friction, the exponential damping is visible. It results in the width $\Gamma = 1.62$ MeV of the frequency spectrum. The peak position of the frequency spectrum is 14.21 MeV, which is the same as that in Fig. 1(d). The friction and random forces do not affect the ISGMR energy.

The model is applied to calculate the excitation energies and widths of the ISGMR in nuclei from ^{12}C to ^{238}U. The results are shown in Fig. 3, and compared to the data and calculations by other models. It is well known from the empirical systematic study that the ISGMR energies approximately follow the relation of $E^* = \eta\, A^{-1/3}$ [2]. The $A^{-1/3}$ law can be deduced

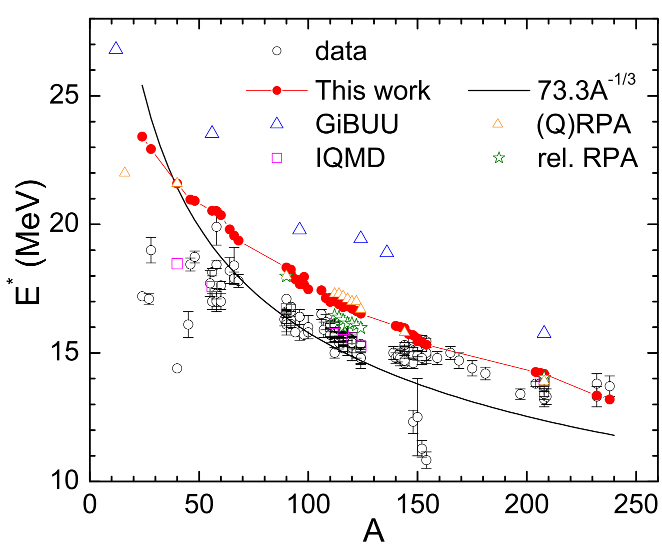

FIG. 3. Excitation energies of the ISGMR as a function of the mass number. In the calculation, the Skyrme force Sky5 is applied. The solid line shows the fit by $A^{-1/3}$ law. The calculations by the relativistic RPA with FSUGold interaction are taken from Ref. [25]. The calculations by (Q)RPA model with Skyrme interaction T6 are taken from Ref. [24]. The calculations by GiBUU model are taken from Ref. [30]. The IQMD results are taken from Ref. [29]. Experimental data are from Refs. [7,11].

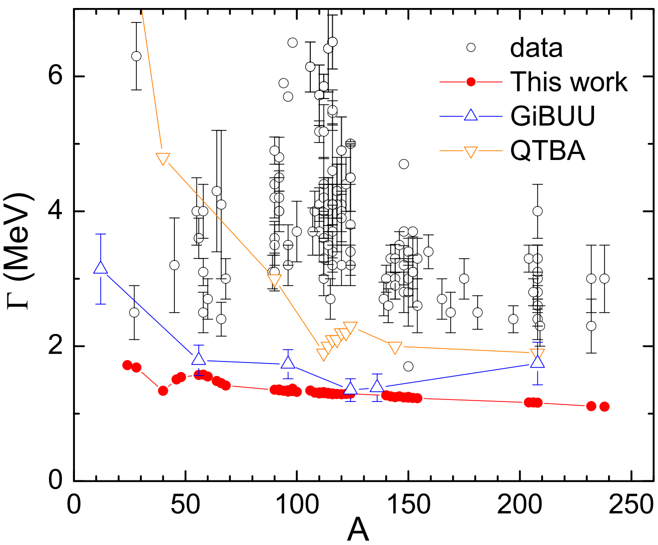

FIG. 4. Same as Fig. 3 but for the width of the ISGMR. The calculations by QTBA is taken from Ref. [24].

by the soundlike excitation in a finite system [1],

$$\begin{aligned} E^* &= \hbar v_s k, \\ v_s &= \sqrt{\frac{K}{9m}}, \\ k &= \frac{\pi}{R} = \frac{\pi}{1.2A^{1/3}}, \end{aligned} \tag{12}$$

where v_s is the sound velocity, k is the eigenvalue of the lowest compressional model, m is the mass of the nucleon, and K is the incompressibility. By the best fit of the data, $\eta = 73.3$ MeV, i.e., $K = 170$ MeV is obtained. The $A^{-1/3}$ law fitting is shown as a black curve in Fig. 3. In fact, the $A^{-1/3}$ law is only the zeroth-order approximation, in which both the isospin effect and surface effect are not considered. Thus, one sees the deviation between the data and the $A^{-1/3}$ law fit. Several models have been applied to calculate the mass dependence of the ISGMR energies. Two transport models, Giessen BUU (GiBUU) and IQMD, provide calculations with visible difference. In the IQMD calculations, which globally agree to the data, the Gaussian wave-packet width is used as the fitting parameter. Our model reproduces the ISGMR energies of ^{208}Pb, ^{232}Th, and ^{238}U, but overestimates those of lighter nuclei, which is consistent with two microscopic approaches [relativistic RPA and (Q)RPA]. The nuclear interactions used in three models, i.e., FSUGold in relativistic RPA, Skyrme T6 in (Q)RPA, and Skyrme Sly5 in this work, provide the incompressibility for symmetric nuclear matter of $K_\infty = 230$ MeV. Comparing to the relativistic RPA and (Q)RPA models, our model provides a method to understand the ISGMR macroscopically.

The damping of a collective vibration, which results in the width, is related to the dissipation processes. The calculations by the GiBUU model have shown that both one-body and two-body dissipation contribute to the widths of the ISGMR [30].

In the reduction of the Boltzmann-Langevin equation in this work, only the two-body dissipation is included [31]. Hence, one sees the smaller widths of the ISGMR predicted by our

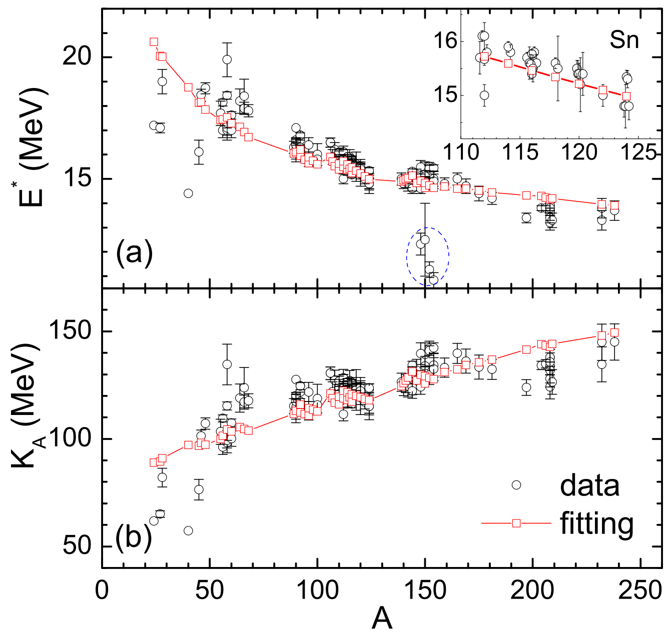

FIG. 5. Excitation energy E^* (top) and incompressibility K_A (bottom) of the ISGMR as a function of the mass number. The inset panel at the top shows E^* of Sn isotopes. Experimental data are from Refs. [7,11].

model as compared to GiBUU. Using the quasiparticle time blocking approximation (QTBA), the damping mechanism is included in the (Q)RPA model. This mechanism results in larger widths, however it still can not reproduce the data for heavy nuclei.

B. Incompressibility in finite nuclei

The incompressibility K_A of a finite nucleus is defined using the ISGMR energy [3],

$$K_A = \frac{m}{\hbar^2}\langle r^2\rangle E^{*2}, \tag{13}$$

where $\langle r^2\rangle$ is the mean-square radius of the nucleus. The experimental data of ISGMR energies, together with the empirical formula $\langle r^2\rangle^{1/2} = 0.82A^{1/3} + 0.58$ from Ref. [37] is applied to calculate the K_A values. The results are show in Fig. 5. The K_A values increase with increasing mass number, and reach 145 MeV for ^{238}U. The incompressibility K_A of the finite nucleus is smaller than that of the infinite nuclear matter, $K_\infty = 230 \pm 40$ MeV.

In analogy to the liquid-drop formula for the nuclear masses, the finite nucleus incompressibility K_A is related to the nuclear matter incompressibility K_∞, i.e., the so-called leptodermous expansion [3],

$$K_A = K_\infty + K_S A^{-1/3} + K_\tau \delta^2 + K_C \frac{Z^2}{A^{4/3}}, \tag{14}$$

where $\delta = (N - Z)/A$ is the neutron-proton asymmetry, Z and N are the charge number and neutron number, K_S, K_τ, and K_C are the surface, symmetry, and Coulomb incompressibility parameters, respectively. The parameters are determined by fitting the experimental data. In the fitting, $K_\infty = 230$ MeV is

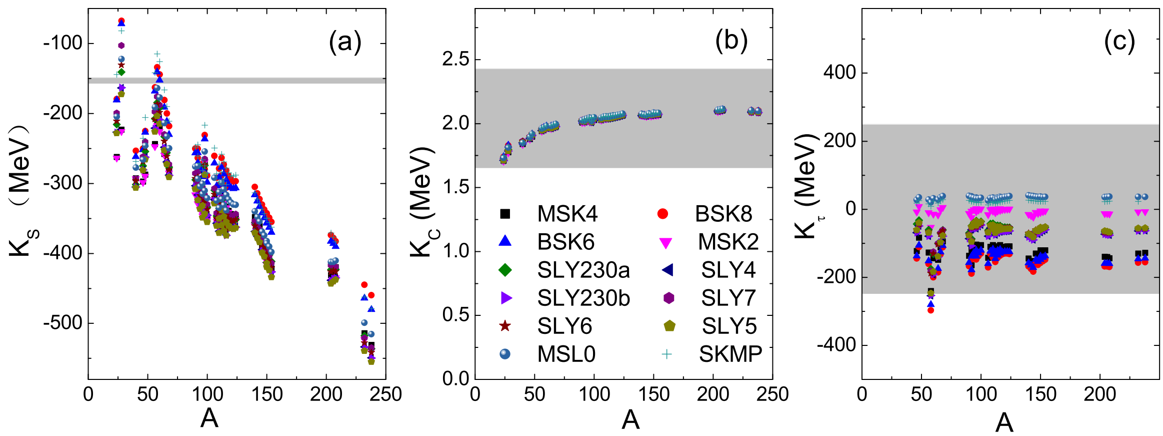

FIG. 6. Surface parameter K_S, symmetry parameter K_τ, and Coulomb parameter K_C of the incompressibility as a function of the mass number.

unadjusted in order to compare with the following calculations, in which Skyrme interactions providing $K_\infty = 230$ MeV are applied. The data deviating from the systematics, which are shown in the dashed circle in Fig. 5, are not used. It is obtained that $K_S = -153.2 \pm 4.7$ MeV, $K_\tau = 0.0 \pm 205.1$ MeV, and $K_C = 2.0 \pm 0.4$ MeV. Those parameters can reproduce the ISGMR energies of Sn isotopes reasonably well, as shown in the inset panel in Fig. 5.

Starting from the Langevin equation Eq. (3), the incompressibility parameters can be calculated. After linearization, Eq. (3) becomes,

$$M^{(0)}\ddot{X} + X\big[3V_c^{(0)} + 8E_k^{(0)} + 15V_0^{(0)} + (3+3\sigma)(5+3\sigma)V_3^{(0)} + 35V_{\rm eff}^{(0)} + 35V_{\rm fin}^{(0)} + 35V_{\rm so}^{(0)} + 35V_{\rm sg}^{(0)}\big] = 0, \quad (15)$$

and leads to the solution,

$$E^* = \hbar\sqrt{\frac{K_A}{m\langle r^2\rangle}},$$

$$K_A = \frac{1}{A}\big[3V_c^{(0)} + 8E_k^{(0)} + 15V_0^{(0)} + (3+3\sigma)(5+3\sigma)V_3^{(0)} + 35V_{\rm eff}^{(0)} + 35V_{\rm fin}^{(0)} + 35V_{\rm so}^{(0)} + 35V_{\rm sg}^{(0)}\big]. \quad (16)$$

The mean-square radius, the Skyrme potential energy, and the kinetic energy are calculated by the SHFB model. That is to say, we can calculate the ISGMR energy and finite nucleus incompressibility K_A directly by the SHFB model. It is interesting to point out that the two-body term V_0 does not contribute to the nuclear matter incompressibility K_∞, but contributes to the finite nucleus incompressibility K_A.

Comparing Eq. (16) to Eq. (14), the incompressibility parameters K_S, K_τ, and K_C are obtained. The $V_c^{(0)}$ term contributes to the Coulomb incompressibility parameter,

$$K_C = \frac{3V_c^{(0)}}{A}\frac{A^{4/3}}{Z^2}. \quad (17)$$

Assuming $\rho_n = \rho_p$, $\tau_n = \tau_p$, and $J_n = J_p$ with keeping the total density constant, we calculate the incompressibility for symmetry system $K_A(\delta = 0)$. The symmetry parameter K_τ is calculated by

$$K_\tau = \frac{1}{\delta^2}[K_A - K_A(\delta = 0)]. \quad (18)$$

Then, the surface parameter K_S is calculated from K_A, K_C, and K_τ,

$$K_S = A^{1/3}\left[K_A - K_\infty - K_\tau\delta^2 - K_C\frac{Z^2}{A^{4/3}}\right]. \quad (19)$$

We perform the SHFB calculations for the nuclei from ^{12}C to ^{238}U within 12 sets of the Skyrme parameters, MSk2, MSk4, BSk6, BSK8, SLy4, SLy5, SLy6, SLy7, SLy230a, SLy230b, MSL0, SkMP. The nuclear matter incompressibilities provided by those Skyrme parameters are in the region from 229–231 MeV. The incompressibility parameters are calculated and shown as a function of mass number in Fig. 6. In the figure, the incompressibility parameters (upper and lower limits) extracted from the data are shown as gray region.

For the surface parameter K_S, the extracted value by the data is -153.2 ± 4.7 MeV. However, the calculations are in the region from -100 to -600 MeV. It has been shown above that the model overestimates the data of the ISGMR energies for $A < 150$. The underestimation of the surface parameter K_S is the result of the overestimation of the ISGMR energies. Moreover, the calculated K_S value decreases linearly over mass number. It is indicated that the data could be better described if the $A^{2/3}$ scaling term is added in the liquid-drop formula Eq. (14).

For the Coulomb parameter K_C, the extracted value from the data is 2.0 ± 0.4 MeV, while the calculated values are in the region from 1.7–2.1 MeV. Although the calculated values slightly depend on the mass number, they are in the confidence interval of the extracted value. In fact, the Coulomb parameter K_C has been studied widely. In those investigations, the negative term related to the third derivative of the energy per nucleon over density is considered. Our model does not consider the third derivative of the energy per nucleon, but can reproduce the extracted value from the data.

Many attempts to extract the symmetry parameter K_τ were based on the data of the Sn and Cd isotopes. The value about -550 MeV was obtained [11]. However, the ISGMR energies of the Sn and Cd isotopes are not only isospin dependent but also mass dependent. The extracted symmetry parameter K_τ depends on the assumed mass dependence of the ISGMR energies. Two evidences support this point of view. First, the value $K_\tau = -550$ MeV can not explain the isospin dependence of the ISGMR in light nuclei, such as Ca isotopes [19]. Second, the value $K_\tau = 0$ MeV, extracted from the data for nuclei from ^{12}C to ^{238}U, can reproduce the ISGMR energies of Sn isotopes reasonably, as shown in the inset panel in Fig. 5. The symmetry parameter K_τ can be also extracted from the data of isobars. In this case, the mass effect can be removed. Unfortunately, the error bars of available isobars data, such as ^{112}Sn-^{112}Cd, ^{114}Sn-^{114}Cd, and ^{116}Sn-^{116}Cd, are too large to constrain the K_τ value. Equation (18) provides a method to calculate K_τ. The calculated values locate in the region from -200 to 50 MeV, which is narrower than the region of the extracted value (0 ± 205.1 MeV). The extracted and calculated values in this work are both much smaller than -550 MeV, but they agree with each other.

IV. CONCLUSION

The fluid dynamical reduction of the Boltzmann-Langevin equation was carried out for a situation where the velocity field can be described by a set of N collective variables [31,32]. In this work, the deducing Langevin equation is applied to investigate the isoscalar giant monopole resonance (ISGMR). It is shown that the calculations of the ISGMR energies in this work agree with those of the relativistic mean-field theory and the random phase approximation, and reproduce the general trend of the data. The model only includes the two-body dissipation, and hence underestimates the width of the ISGMR.

By linearization of the Langevin equation, a method is provided to calculate the incompressibility K_A of the finite nucleus directly by the Skyrme Hartree-Fock-Bogolyubov model. Twelve sets of the Skyrme interactions are applied to perform the calculations and study the incompressibility parameters in the leptodermous expansion. The incompressibility parameters are also extracted by fitting the available data for the nuclei from ^{12}C to ^{238}U. For the surface parameter K_S, the extracted value by the data is -153.2 ± 4.7 MeV. Because of the overestimation of the ISGMR energies by the model, the calculated K_S values are smaller than the extracted value, and decrease linearly over mass number of the nucleus.

The calculated K_C values (1.7–2.1 MeV) agree with the extracted value (2.0 ± 0.4 MeV). For the symmetry parameter K_τ, the extracted value is 0 with a large uncertainty ± 205.1 MeV. The calculated values locate in the region from -200 to 50 MeV, which is narrower than the region of the extracted value. The Bohr-Mottelson model provides a reasonable method to understand the ISGMR macroscopically. With more data of the ISGMR in short-lived nuclei in the future, it will be used to constrain the incompressibility parameters, especially the symmetry part.

ACKNOWLEDGMENTS

This work was supported by the National Natural Science Foundation of China under Grants No. 11405278, No. 11605296, and No. 11605270, and the Natural Science Foundation of Guangdong Province China under Grant No. 2016A030310208.

[1] A. Bohr and B. Mottelson, *Nuclear Structure* (Benjamin, New York, 1975), Vol. 2.
[2] M. N. Harakeh and A. van der Woude, *Giant Resonances Fundamental High-Frequency Modes of Nuclear Excitation, Excitation* (Oxford University Press, New York, 2001).
[3] J. Blaizot, Phys. Rep. **64**, 171 (1980).
[4] S. Brandenburg, R. DeLeo, A. G. Drentje, M. N. Harakeh, H. Janszen, and A. van der Woude, Phys. Rev. Lett. **49**, 1687 (1982).
[5] F. Zwarts, A. Drentje, M. Harakeh, and A. van der Woude, Phys. Lett. B **125**, 123 (1983).
[6] S. Brandenburg, R. D. Leo, A. Drentje, M. Harakeh, H. Sakai, and A. van der Woude, Phys. Lett. B **130**, 9 (1983).
[7] S. Shlomo and D. H. Youngblood, Phys. Rev. C **47**, 529 (1993).
[8] D. H. Youngblood, H. L. Clark, and Y.-W. Lui, Phys. Rev. Lett. **82**, 691 (1999).
[9] S. Shlomo, V. M. Kolomietz, and G. Colò, Eur. Phys. J. A **30**, 23 (2006).
[10] E. Khan, J. Margueron, and I. Vidaña, Phys. Rev. Lett. **109**, 092501 (2012).
[11] U. Garg and G. Colò, Prog. Part. Nucl. Phys. **101**, 55 (2018).
[12] T. Li, U. Garg, Y. Liu, R. Marks, B. K. Nayak, P. V. Madhusudhana Rao, M. Fujiwara, H. Hashimoto, K. Kawase, K. Nakanishi, S. Okumura, M. Yosoi, M. Itoh, M. Ichikawa, R. Matsuo, T. Terazono, M. Uchida, T. Kawabata, H. Akimune, Y. Iwao, T. Murakami, H. Sakaguchi, S. Terashima, Y. Yasuda, J. Zenihiro, and M. N. Harakeh, Phys. Rev. Lett. **99**, 162503 (2007).
[13] D. Patel, U. Garg, M. Fujiwara, H. Akimune, G. Berg, M. Harakeh, M. Itoh, T. Kawabata, K. Kawase, B. Nayak, T. Ohta, H. Ouchi, J. Piekarewicz, M. Uchida, H. Yoshida, and M. Yosoi, Phys. Lett. B **718**, 447 (2012).
[14] J. Piekarewicz, Phys. Rev. C **76**, 031301 (2007).
[15] G. Colò, N. V. Giai, J. Meyer, K. Bennaceur, and P. Bonche, Phys. Rev. C **70**, 024307 (2004).
[16] P. Avogadro and C. A. Bertulani, Phys. Rev. C **88**, 044319 (2013).
[17] T. Peach, U. Garg, Y. K. Gupta, J. Hoffman, J. T. Matta, D. Patel, P. V. Madhusudhana Rao, K. Yoshida, M. Itoh, M. Fujiwara, K. Hara, H. Hashimoto, K. Nakanishi, M. Yosoi, H. Sakaguchi, S. Terashima, S. Kishi, T. Murakami, M. Uchida, Y. Yasuda, H. Akimune, T. Kawabata, M. N. Harakeh, and G. Colò, Phys. Rev. C **93**, 064325 (2016).
[18] Y. Gupta, U. Garg, J. Matta, D. Patel, T. Peach, J. Hoffman, K. Yoshida, M. Itoh, M. Fujiwara, K. Hara, H. Hashimoto, K. Nakanishi, M. Yosoi, H. Sakaguchi, S. Terashima, S. Kishi, T. Murakami, M. Uchida, Y. Yasuda, H. Akimune, T. Kawabata, and M. Harakeh, Phys. Lett. B **748**, 343 (2015).
[19] J. Button, Y.-W. Lui, D. H. Youngblood, X. Chen, G. Bonasera, and S. Shlomo, Phys. Rev. C **96**, 054330 (2017).

[20] C. Monrozeau, E. Khan, Y. Blumenfeld, C. E. Demonchy, W. Mittig, P. Roussel-Chomaz, D. Beaumel, M. Caamaño, D. Cortina-Gil, J. P. Ebran, N. Frascaria, U. Garg, M. Gelin, A. Gillibert, D. Gupta, N. Keeley, F. Maréchal, A. Obertelli, and J.-A. Scarpaci, Phys. Rev. Lett. **100**, 042501 (2008).

[21] P. Veselý, J. Toivanen, B. G. Carlsson, J. Dobaczewski, N. Michel, and A. Pastore, Phys. Rev. C **86**, 024303 (2012).

[22] J. R. Stone, N. J. Stone, and S. A. Moszkowski, Phys. Rev. C **89**, 044316 (2014).

[23] P. S. P. Ring, *The Nuclear Many-Body Problem* (Springer Verlag, New York, 1980).

[24] V. Tselyaev, S. Krewald, E. Litvinova, and J. Speth, arXiv:0912.5328v2.

[25] J. Piekarewicz and M. Centelles, Phys. Rev. C **79**, 054311 (2009).

[26] M. Sharma, Nucl. Phys. A **816**, 65 (2009).

[27] L.-G. Cao, H. Sagawa, and G. Colò, Phys. Rev. C **86**, 054313 (2012).

[28] D. Gambacurta, M. Grasso, and J. Engel, Phys. Rev. C **92**, 034303 (2015).

[29] C. Tao, Y. G. Ma, G. Q. Zhang, X. G. Cao, D. Q. Fang, H. W. Wang, and J. Xu, Phys. Rev. C **88**, 064615 (2013).

[30] T. Gaitanos, A. B. Larionov, H. Lenske, and U. Mosel, Phys. Rev. C **81**, 054316 (2010).

[31] S. Ayik, E. Suraud, J. Stryjewski, and M. Belkacem, Z. Phys. A **337**, 413 (1990).

[32] D. Boilley, Y. Abe, S. Ayik, and E. Suraud, Z. Phys. A **349**, 119 (1994).

[33] D. Vautherin and D. M. Brink, Phys. Rev. C **5**, 626 (1972).

[34] J. Dechargé and D. Gogny, Phys. Rev. C **21**, 1568 (1980).

[35] M. Brack, C. Guet, and H.-B. Håkansson, Phys. Rep. **123**, 275 (1985).

[36] K. Bennaceur and J. Dobaczewski, Comput. Phys. Commun. **168**, 96 (2005).

[37] M. A. Preston and R. K. Bhaduri, *Structure of the Nucleus* (Addison-Wesley, Reading, 1975), pp. 1014.